VIP Nanowires Very Important Paper

International Edition: DOI: 10.1002/anie.201412388
German Edition: DOI: 10.1002/ange.201412388

Flow-Enabled Self-Assembly of Large-Scale Aligned Nanowires**

*Bo Li, Chuchu Zhang, Beibei Jiang, Wei Han, and Zhiqun Lin**

Abstract: *One-dimensional nanowires enable the realization of optical and electronic nanodevices that may find applications in energy conversion and storage systems. Herein, large-scale aligned DNA nanowires were crafted by flow-enabled self-assembly (FESA). The highly oriented and continuous DNA nanowires were then capitalized on either as a template to form metallic nanowires by exposing DNA nanowires that had been preloaded with metal salts to an oxygen plasma or as a scaffold to direct the positioning and alignment of metal nanoparticles and nanorods. The FESA strategy is simple and easy to implement and thus a promising new method for the low-cost synthesis of large-scale one-dimensional nanostructures for nanodevices.*

The past decade has witnessed remarkable progress in the chemical synthesis and lithographic fabrication of nanowires with unique size-dependent optical and electronic properties.[1] They have emerged as an important class of nanomaterials that are used as building blocks and interconnecting units for nanodevices and have found application in energy conversion and storage systems.[2] For example, silicon nanowires are employed as new light-harvesting semiconductors for solar energy conversion.[3] Compared with TiO_2 nanoparticles, the use of an array of densely packed TiO_2 nanowires as the photoanode provides a direct pathway for charge transport from the point of injection to the collecting electrode while retaining a large surface area for dye loading in dye-sensitized solar cells (DSSCs).[4] The synthesis of chemically grown nanowires in industry is often rather expensive, and these nanostructures tend to exhibit relatively weak adhesion to the substrate. On the other hand, lithographic techniques enable the synthesis of nanowires with controlled sizes and well-defined growth locations on the substrate, but often require an iterative multistep procedure that is time-consuming and expensive. Clearly, it is of great interest and technological importance to explore inexpensive non-lithographic strategies for the synthesis of long nanowires.

In this context, the use of biotemplates (e.g., viruses,[5] peptides,[6] and DNA[7]) offers a promising route to one-dimensional nanomaterials.[8] In particular, DNA has been widely recognized as an ideal biotemplate for creating a broad range of metallic nanowires[9] owing to its remarkably high aspect ratio (with a diameter of 2 nm and a length of tens of micrometers). However, the dramatic increase in stiffness and significant aggregation between metallized DNA molecules make it difficult to immobilize and precisely position metallized DNA molecules on a solid substrate.[9b] Furthermore, the length of the metallic nanowires thus obtained is only a few tens of micrometers. However, longer metallic nanowires are highly desirable for a range of practical applications.[10] Obviously, the key to achieving well-ordered and continuous metallic nanowires is to first produce regularly aligned DNA nanowires on a substrate, which are subsequently subjected to metallization. However, it remains challenging to achieve highly ordered and continuous DNA nanowires on a substrate. Notably, a single flexible DNA molecule can be stretched and aligned using a receding meniscus (a "molecular combing" method).[11] Similar approaches to stretched DNA have also been developed, including microchannel combing,[12] air-blow combing,[13] spin stretching,[14] and electric-field-assisted combing.[15] Nonetheless, the immobilized individual DNA molecules are often randomly positioned, and the ability of creating long DNA nanowires is very limited in scope.[16] Clearly, the formation of well-positioned continuous DNA nanowires depends critically on the intricate control over solvent evaporation during the combing or stretching of DNA molecules. It is worth mentioning that irregular dissipative patterns of nonvolatile solutes (e.g., polymers, colloids, nanoparticles, or carbon nanotubes) are commonly observed for the evaporation of sessile droplets owing to flow instabilities within the drying droplet.[17] By delicately controlling the evaporation process (e.g., the evaporative flux, the solution concentration, and the interfacial interaction between solute and substrate),[18] for example, by constructing curve-on-flat geometries to constrain and regulate solvent evaporation and eliminate the temperature gradient, one- and two-dimensional as well as hierarchical structures and assemblies of polymers[19] and nanoparticles[20] with unprecedented regularity and fidelity have been reproducibly produced.[21]

Herein, we report a simple and viable strategy to achieve large-scale aligned nanowires templated by highly oriented DNA nanowires, which were crafted by flow-enabled self-assembly (FESA). By letting an aqueous solution of DNA dry between two nearly parallel plates, that is, a stationary upper plate and a movable lower plate mounted on a programmable translational stage (in a FESA process), an array of ultralong, parallel, and dense DNA nanowires on a large scale was successfully created. The positions of the DNA nanowire deposits were fixed on the substrate through the anchoring of the DNA extremities onto the hydrophobic substrate. The formation of DNA nanowires was strongly influenced by the concentration of the DNA solution, the temperature, and the moving speed of the lower plate. The length of the highly oriented DNA nanowires was simply dictated by the amount

[*] B. Li, C. Zhang, B. Jiang, Dr. W. Han, Prof. Z. Lin
School of Materials Science and Engineering
Georgia Institute of Technology
Atlanta, GA 30332 (USA)
E-mail: zhiqun.lin@mse.gatech.edu

[**] We gratefully acknowledge support from the NSF (CBET-1332780).
Supporting information for this article is available on the WWW under http://dx.doi.org/10.1002/anie.201412388.

of DNA solution used in the FESA process. A simple, yet robust swelling-induced transfer printing (SIT printing) technique was developed to transfer the ultralong DNA nanowires onto a desirable substrate. Subsequently, the resulting DNA nanowires were exploited as templates for the formation of metallic nanowires by subjecting DNA nanowires preloaded with metal salts to oxygen plasma. Moreover, the DNA nanowires were also employed as scaffold materials for aligning metal nanoparticles and nanorods. The ability of placing DNA into one-dimensional, parallel, and continuous nanowire arrays, in combination with their use as templates for functional inorganic nanostructures, may enable the mass production of integrated nanodevices.

A drop of an aqueous solution containing YOYO-1-labeled DNA was loaded into a confined geometry comprising a lower movable PDMS substrate and an upper stationary glass plate separated by 300 μm (Figure 1a). The lower

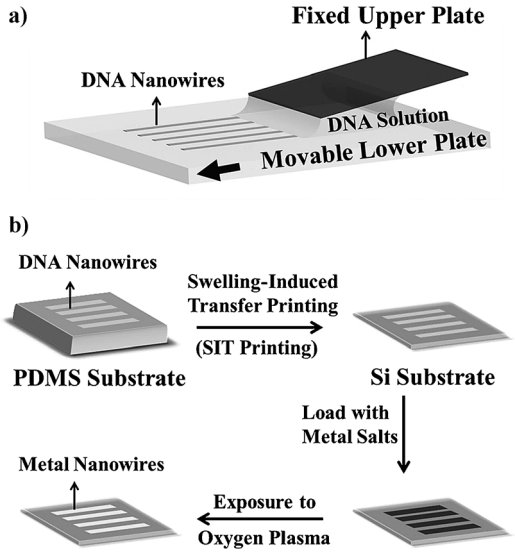

Figure 1. a) Schematic illustration of crafting an array of high-density continuous DNA nanowires by flow-enabled self-assembly (FESA). The DNA solution was constrained between two nearly parallel plates with the lower PDMS substrate placed on a translation stage moved against the upper fixed glass plate. b) Schematic representation of the SIT printing of DNA nanowires and the subsequent metallization of DNA nanowires by exposing DNA nanowires preloaded with metal salts to oxygen plasma.

substrate was mounted on a translational stage controlled by a computer (see the Supporting Information). The DNA molecules were first transported to the three-phase contact line (i.e., the air/water/substrate interface; receding meniscus) owing to the evaporative loss of water.[17a,22] As the lower PDMS substrate was subsequently moved, fingering instabilities emerged at the drying front owing to unfavorable interactions between DNA and PDMS (i.e., van der Waals forces).[23] Over a certain range of pH values, the partial melting of the ends or extremities of DNA molecules exposes their hydrophobic core, which can then adsorb onto a hydrophobic surface (i.e., specific binding).[12,24] Such anchoring was strong enough to withstand the dragging force exerted by the motion of the PDMS substrate. Thus, the DNA molecules were stretched and aligned along the moving direction of the PMDS substrate. The anchored DNA molecules acted as the nucleation sites, to which more DNA molecules were transported and then grown along them, thereby creating continuous DNA nanowires with a length of one centimeter (Figure 1a). Notably, much longer DNA nanowires were easily attainable by using a larger amount of the DNA solution (> 60 μL) and increasing the moving distance of the PDMS substrate (> 1 cm; see the Supporting Information). It is not surprising that as the DNA molecules were stretched perpendicularly with respect to the evaporating front, an array of parallel and continuous DNA nanowires with a length on the centimeter scale were thus readily obtained.

Intriguingly, the formation of highly aligned DNA nanowires depended strongly on the DNA concentration, the temperature, and the moving speed of the PDMS substrate (Figure 2). For the crafting of long and continuous DNA nanowires, there is an optimal range of deposition density of DNA molecules (Figure 2b). A higher deposition density led to the formation of branched DNA bundles (Figure 2a), whereas a lower deposition density resulted in the production of discontinuous DNA lines (i.e., short stripes; Figure 2c). To tailor the deposition density of DNA, the concentration of the DNA solution, the temperature, the pH value of the DNA

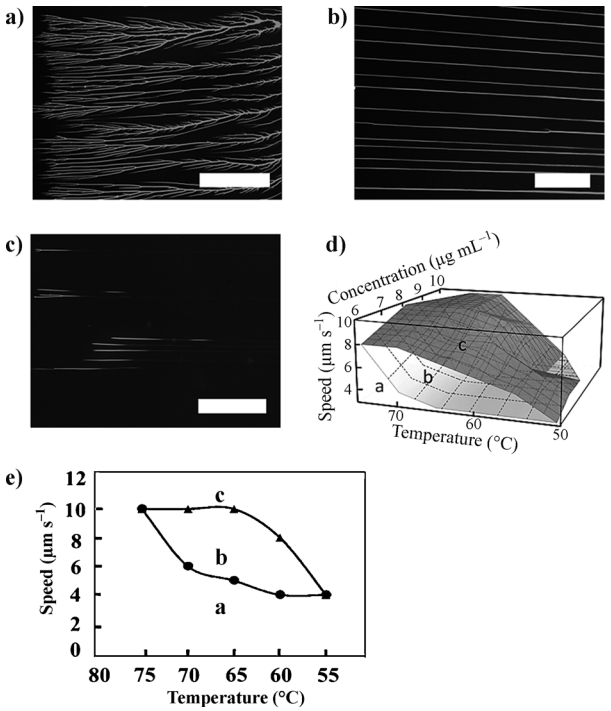

Figure 2. a–c) Representative fluorescence micrographs of self-assembled YOYO-1-labeled DNA molecules: branched DNA bundles (a), continuous DNA nanowires (b), and short DNA lines (c). Scale bars: 500 μm (a and c); 100 μm (b). d) 3D map showing the dependence of the formed DNA pattern on the DNA concentration, the moving speed of the PDMS substrate, and the temperature. The labels a, b, and c correspond to the range of experimental conditions that yield the DNA nanostructures shown in (a), (b) and (c), respectively. e) 2D map of the moving speed of the lower PDMS substrate and of the temperature for DNA pattern formation at a fixed concentration of 8 μg mL^{-1}.

solution, the surface chemistry of the substrate, and the moving speed of the substrate can be adjusted. To this end, we systematically varied the concentration, temperature, and the moving speed of the substrate, while maintaining a constant pH value (i.e., pH 6.2) and using PDMS as the substrate. Obviously, a higher concentration of the DNA solution and a reduced moving speed of the PDMS substrate would bring about a larger deposition. Moreover, an increase in temperature would induce a higher evaporation rate at the receding meniscus, thereby transporting more DNA molecules to the three-phase contact line, where they are deposited. The judicious combination of these three variables that enabled the formation of long and continuous DNA nanowires is represented by area b in Figure 2d, enveloped by the upper boundary (above which short DNA lines were formed as marked with c in Figure 2d, corresponding to the optical micrograph in Figure 2c) and the lower boundary (below which branched DNA bundles were formed as marked with a in Figure 2d, corresponding to the optical micrograph in Figure 2a). Figure 2e shows a representative temperature/moving speed plot at a DNA concentration of 8 $\mu g\,mL^{-1}$. The temperature/moving speed plots at other concentrations are shown in the Supporting Information, Figure S1. Notably, there existed a critical range of DNA concentration for the formation of the DNA nanowires (5–14 $\mu g\,mL^{-1}$; not shown in Figure 2d and Figure S1). At higher concentrations ($>14\ \mu g\,mL^{-1}$), either branched DNA bundles, short DNA lines, or a mixture of both were obtained as the deposits depending on the temperature and the moving speed of the PDMS substrate. At lower concentrations ($<5\ \mu g\,mL^{-1}$), only few DNA molecules were deposited on the substrate, and thus only short DNA lines were formed. With the FESA process, large-scale continuous DNA nanowires could be attained over a much wider temperature range (55–75 °C; Figure 2e) than with previously reported methods[19a] (see the Supporting Information).

A prerequisite of using DNA as a template for the synthesis of inorganic nanostructures is the ability to transfer-print DNA nanowires onto the desirable substrate (e.g., from the PDMS substrate to a Si wafer). Unfortunately, we found that the conventional "contact and peel off" method[25] was not applicable to transfer-printing the as-prepared DNA nanowires from the PDMS to the Si substrate as only a few DNA nanowires were transferred. Moreover, the originally continuous DNA nanowires were segmented during the transfer-printing process. One possible reason may be that the adhesion between the DNA nanowires and the PDMS substrate is stronger than for a single DNA molecule anchored on the PDMS substrate[25] owing to the larger contact area between the DNA nanowires and the PDMS substrate in the present study. To this end, we developed a facile swelling-induced transfer printing (SIT printing) approach to transfer the DNA nanowires, as schematically illustrated in Figure S2. First, the PDMS substrate with deposited DNA nanowires was brought into contact with a Si wafer immediately after it had been crafted by the FESA process. The DNA nanowire modified PDMS/Si substrate was then immersed in toluene. As PDMS swelled in toluene, the PDMS substrate was gradually detached from the Si substrate and floated on top of the toluene solution. The DNA nanowires, however, remained and were transferred onto the Si substrate on the bottom of the toluene. The entire SIT printing process was completed in 20 minutes. Interestingly, DNA nanowires that have been transferred onto the Si substrate can be preserved in toluene for days as toluene is a non-solvent for DNA. Furthermore, we anticipate that by carrying out two orthogonal SIT printing processes, two-dimensional meshes of DNA nanowires should be achievable.

To scrutinize and better understand this intriguing and effective SIT printing process, we simply added a drop of toluene (20 μL) to the DNA nanowire coated PDMS substrate that was described above. The DNA nanowires could be easily lifted off the PDMS substrate without destroying the continuity of the DNA nanowires (Figure S3). It is plausible that toluene diffused into the DNA/PDMS interface and that the PDMS substrate swelled by adsorbing toluene. As DNA is hydrophilic whereas PDMS is hydrophobic, the DNA nanowires thus delaminate from the swollen PDMS substrate. Similarly, during SIT printing, toluene entered the tightly contacted DNA nanowire-deposited PDMS/Si interface and facilitated the detachment of the DNA nanowires from the PDMS substrate and their transferal to the Si substrate as both the Si substrate and the DNA nanowires are hydrophilic. Furthermore, the swollen PDMS in toluene may also exert a uniform pressure on the Si substrate to promote the transfer printing.

Subsequently, conductive metal nanowires were produced by exploiting DNA nanowires that had been transferred onto a Si substrate by SIT printing as a template. Despite several studies on the metallization of single DNA molecules in solution,[8,10,26] the reported methods could not be extended to metalize continuous DNA nanowires in the solid state. This is likely due to the difficulties associated with metallizing DNA nanowires while retaining the self-assembled DNA nanostructures on the substrate. It is easy to understand that as water is used as the solvent of the metal precursor solution, the DNA nanowires will be dissolved by water once the precursor water solution has been added to the DNA nanowires. Therefore, in order to load metal salts onto the DNA nanowires, a non-solvent for DNA is needed when preparing the metal precursor solution. In this work, a silver precursor solution ($AgNO_3$) was prepared in a mixed solvent system (DMF/toluene = 1:1, v/v). The Si substrate with deposited DNA nanowires was then immersed into the $AgNO_3$ solution in DMF/toluene for 24 hours. Because of the electrostatic attraction between the positively charged Ag^+ ions and the negatively charged DNA backbone, the Ag^+ ions were bound to the DNA. DNA nanowires preloaded with metal salts were thus produced. Conventionally, the chemical reduction of silver precursors leads to the formation of Ag nanowires. However, we found that the reducing agent needed to be carefully selected. For example, the addition of a strong reductant, such as tetra-*n*-butylammonium bromide (TBAB), to the soaking solution caused not only the instant formation of Ag nanowires, but also the unwanted deposition of Ag nanoparticles all over the substrate (Figure 3a).

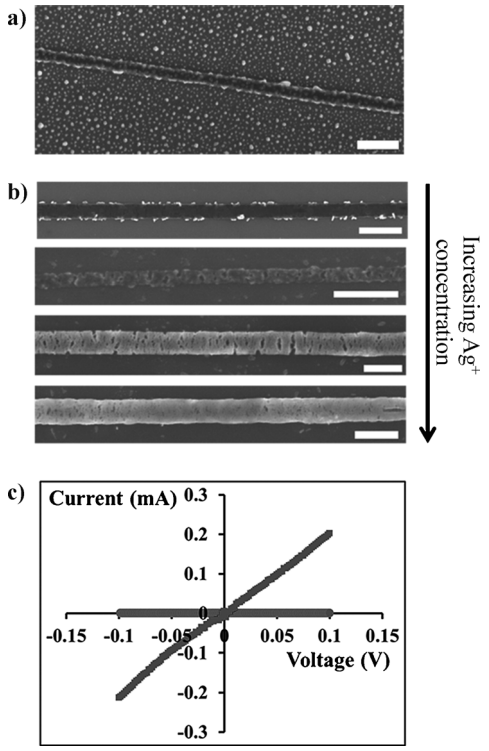

Figure 3. Representative SEM image of Ag nanowires formed a) by chemical reduction with Ag nanoparticles deposited all over the surface, and b) by a reduction induced by oxygen plasma for various $AgNO_3$ concentrations (top to bottom: 0.5, 1, 10, and 50 mg mL^{-1}). c) Current–voltage (*I*–*V*) characteristics of Ag nanowires obtained from DNA nanowires that were preloaded with $AgNO_3$ precursors (50 mg mL^{-1}; sloping line: continuous nanowire; horizontal line: discontinuous nanowire). All scale bars: 400 nm.

Thus, we capitalized on an effective approach to create Ag nanowires by exposing the DNA nanowires loaded with the Ag precursor to oxygen plasma (Figure 3b and Figure S4); the reduction of the Ag^+ precursor ions is enabled by electrons from the oxygen plasma.[27] Moreover, no excess Ag nanoparticles were deposited between adjacent Ag nanowires on the Si substrate as the substrate was washed with toluene and blow-dried prior to the oxygen plasma treatment. Interestingly, the morphology of the grown Ag nanowire was related to the $AgNO_3$ concentration. A lower $AgNO_3$ concentration (0.5 mg mL^{-1}) gave rise to only partially metallized DNA nanowires. At concentrations above 10 mg mL^{-1}, continuous Ag nanowires were formed. The conductivity of the obtained Ag nanowires was then measured (Figure 3c) and found to be much higher for continuous Ag nanowires (sloping line) than for nanowires grown from a single DNA molecule,[7a] as the diameter of a DNA nanowire is larger than that of a single DNA molecule. When the Ag nanowire was cut apart with a razor blade, no current was observed (horizontal line).

DNA nanowires cannot only be used as templates for the formation of metal nanowires, but they can also serve as scaffolds directing the assembly of metal nanoparticles. In this regard, two approaches for producing a nanoparticle assembly were developed. The first approach entails the growth and alignment of the Au nanoparticles along the DNA nanowire by chemical reduction (Figures S5 and S6). Unlike for the growth of Ag nanowires, the Au precursor (i.e., chloroauric acid, $HAuCl_4$) is negatively charged ($AuCl_4^-$) and thus bears the same charge as the backbone of the DNA nanowire. Therefore, after the DNA nanowires had been soaked with the $HAuCl_4$ solution, electrostatic repulsion prevented the binding of $AuCl_4^-$ ions to the DNA backbone. However, the addition of cetyltrimethylammonium bromide (CTAB; a ligand that caps the Au nanoparticle surface) led to the formation of CTAB-functionalized Au nanoparticles from the precursor solution, which were then bonded to the DNA nanowires through electrostatic attractions between the CTAB-functionalized Au nanoparticles with a positively charged surface and the negatively charged DNA backbone. The Au precursor solution with a concentration of 1 mg mL^{-1} was prepared by adding $HAuCl_4$ (10 mg) and CTAB (0.7289 g, 0.2 M) into a mixture of DMF and MeOH (10 mL, DMF/MeOH = 1:1, v/v). Upon addition of the reducing agent (i.e., sodium citrate), the Au nanoparticles nucleated and grew in solution, while capping with CTAB prevented the aggregation of the Au nanoparticles. Interestingly, the size and shape of the Au nanoparticles that were grown and decorated along the DNA nanowire were highly sensitive to the reducing agent (for example, corroded DNA nanowires were observed when $NaBH_4$ was used as the reductant; Figure S7), the concentration, and the addition of the Ag^+ ions. The size of the Au nanoparticles was found to range from tens to hundreds of nanometers. The shape of the Au nanoparticles also varied, including spherical (Figure S5), sea-urchin-like (Figure S6), and flake-like (Figure S8) nanoparticles, which may find applications in localized surface plasmonic resonance (LSPR) owing to their nanometer size and close proximity.[28] All these merit a detailed study and are currently under investigation.

Instead of using Au precursors as described above, the second approach for the assembly of Au nanocrystals using DNA nanowires entails the use of premade Au nanoparticles and nanorods. There are two means of patterning presynthesized nanocrystals along a DNA nanowire: Either DNA and Au nanocrystals are mixed first and then oriented on the substrate, or the DNA nanowire is patterned first, followed by the alignment of Au nanocrystals along the fixed DNA nanowire on the substrate. We found that the first approach did not work as the DNA aggregated with the Au nanoparticles and precipitated prior to deposition on the substrate. In contrast, with the second approach, Au nanocrystals were successfully aligned on the DNA nanowires. First, Au nanoparticles with a diameter of approximately 20 nm were synthesized using sodium citrate as the reducing agent (Figure S9). Subsequently, DNA nanowires were slowly crafted by FESA (e.g., at the moving speed of 6 μm s^{-1} of the PDMS substrate). Finally, the Au nanoparticles were aligned along the direction of the preformed DNA nanowires by a second FESA process at a much higher speed (e.g., 100 μm s^{-1}; Figure 4). A representative TEM image of the aligned Au nanoparticles is shown in Figure 4a. The average height of the DNA nanowires decorated with Au nanoparticles was approximately 60 nm (Figure 4b). Aside from

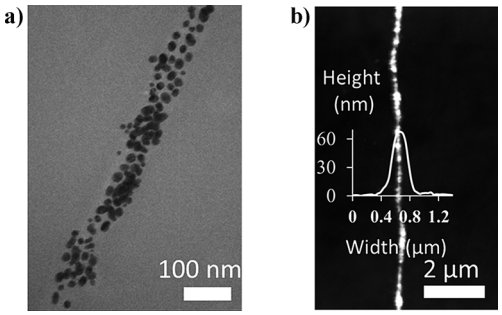

Figure 4. a) Representative TEM image, and b) 2D AFM height image of the direct assembly of premade Au nanoparticles (ca. 20 nm) by employing DNA nanowires as the scaffolds.

Au nanoparticles, Au nanorods could also be aligned along the DNA nanowire (Figure S10).

In summary, we have developed a simple and robust flow-enabled self-assembly strategy for aligning DNA into an array of high-density long nanowires over a large scale. The DNA nanowires were then successfully transferred onto a desirable substrate by a facile swelling-induced transfer printing technique. Subsequently, these parallel and continuous DNA nanowires were exploited either as templates to produce conductive metal nanowires by treatment with oxygen plasma or as scaffolds for the positioning and alignment of metal nanoparticles and nanorods. Clearly, the flow-enabled self-assembly strategy is easy to implement and enables the low-cost synthesis of large-scale one-dimensional polymer- and biomaterial-based nanostructures and their direct exploitation or transformation into useful inorganic nanostructures for their effective integration into nanodevices and the construction of higher hierarchical devices.

Keywords: biotemplates · DNA structures · nanostructures · nanowires · self-assembly

How to cite: *Angew. Chem. Int. Ed.* **2015**, *54*, 4250–4254
Angew. Chem. **2015**, *127*, 4324–4328

[1] R. Yan, D. Gargas, P. Yang, *Nat. Photonics* **2009**, *3*, 569–576.
[2] J. Yuan, Y. Xu, A. Walther, S. Bolisetty, M. Schumacher, H. Schmalz, M. Ballauff, A. H. E. Müller, *Nat. Mater.* **2008**, *7*, 718–722.
[3] A. I. Hochbaum, R. Chen, R. D. Delgado, W. Liang, E. C. Garnett, M. Najarian, A. Majumdar, P. Yang, *Nature* **2008**, *451*, 163–167.
[4] X. Feng, K. Shankar, M. Paulose, C. A. Grimes, *Angew. Chem. Int. Ed.* **2009**, *48*, 8095–8098; *Angew. Chem.* **2009**, *121*, 8239–8242.
[5] K. T. Nam, D.-W. Kim, P. J. Yoo, C.-Y. Chiang, N. Meethong, P. T. Hammond, Y.-M. Chiang, A. M. Belcher, *Science* **2006**, *312*, 885–888.
[6] C.-L. Chen, N. L. Rosi, *Angew. Chem. Int. Ed.* **2010**, *49*, 1924–1942; *Angew. Chem.* **2010**, *122*, 1968–1986.
[7] a) E. Braun, Y. Eichen, U. Sivan, G. Ben-Yoseph, *Nature* **1998**, *391*, 775–778; b) M. Byun, W. Han, B. Li, S. W. Hong, J. W. Cho, Q. Zou, Z. Lin, *Small* **2011**, *7*, 1641–1646.
[8] A. Zinchenko, *J. Polym. Sci. Part C* **2012**, *54*, 80–87.
[9] a) M. Mertig, L. Colombi Ciacchi, R. Seidel, W. Pompe, A. De Vita, *Nano Lett.* **2002**, *2*, 841–844; b) J. Richter, R. Seidel, R. Kirsch, M. Mertig, W. Pompe, J. Plaschke, H. K. Schackert, *Adv. Mater.* **2000**, *12*, 507–510.
[10] H. A. Becerril, A. T. Woolley, *Chem. Soc. Rev.* **2009**, *38*, 329–337.
[11] A. Bensimon, A. Simon, A. Chiffaudel, V. Croquette, F. Heslot, D. Bensimon, *Science* **1994**, *265*, 2096–2098.
[12] C. A. P. Petit, J. D. Carbeck, *Nano Lett.* **2003**, *3*, 1141–1146.
[13] Z. Deng, C. Mao, *Nano Lett.* **2003**, *3*, 1545–1548.
[14] H. Yokota, J. Sunwoo, M. Sarikaya, G. van den Engh, R. Aebersold, *Anal. Chem.* **1999**, *71*, 4418–4422.
[15] F. Dewarrat, M. Calame, C. Schönenberger, *Single Mol.* **2002**, *3*, 189–193.
[16] H. Nakao, T. Taguchi, H. Shiigi, K. Miki, *Chem. Commun.* **2009**, 1858–1860.
[17] a) R. D. Deegan, *Phys. Rev. E* **2000**, *61*, 475–485; b) W. Han, Z. Lin, *Angew. Chem. Int. Ed.* **2012**, *51*, 1534–1546; *Angew. Chem.* **2012**, *124*, 1566–1579; c) B. P. Khanal, E. R. Zubarev, *Angew. Chem. Int. Ed.* **2007**, *46*, 2195–2198; *Angew. Chem.* **2007**, *119*, 2245–2248.
[18] a) S. W. Hong, J. Xia, Z. Lin, *Adv. Mater.* **2007**, *19*, 1413–1417; b) S. W. Hong, J. Wang, Z. Lin, *Angew. Chem. Int. Ed.* **2009**, *48*, 8356–8360; *Angew. Chem.* **2009**, *121*, 8506–8510.
[19] a) B. Li, W. Han, M. Byun, L. Zhu, Q. Zou, Z. Lin, *ACS Nano* **2013**, *7*, 4326–4333; b) W. Han, M. He, M. Byun, B. Li, Z. Lin, *Angew. Chem. Int. Ed.* **2013**, *52*, 2564–2568; *Angew. Chem.* **2013**, *125*, 2624–2628.
[20] J. Xu, J. Xia, Z. Lin, *Angew. Chem. Int. Ed.* **2007**, *46*, 1860–1863; *Angew. Chem.* **2007**, *119*, 1892–1895.
[21] a) M. Byun, W. Han, B. Li, X. Xin, Z. Lin, *Angew. Chem. Int. Ed.* **2013**, *52*, 1122–1127; *Angew. Chem.* **2013**, *125*, 1160–1165; b) M. Byun, N. B. Bowden, Z. Lin, *Nano Lett.* **2010**, *10*, 3111–3117.
[22] J. Xu, J. Xia, S. W. Hong, Z. Lin, F. Qiu, Y. Yang, *Phys. Rev. Lett.* **2006**, *96*, 066104.
[23] I. Leizerson, S. G. Lipson, A. V. Lyushnin, *Langmuir* **2004**, *20*, 291–294.
[24] J. F. Allemand, D. Bensimon, L. Jullien, A. Bensimon, V. Croquette, *Biophys. J.* **1997**, *73*, 2064.
[25] H. Nakao, M. Gad, S. Sugiyama, K. Otobe, T. Ohtani, *J. Am. Chem. Soc.* **2003**, *125*, 7162–7163.
[26] G. Qun, C. Chuanding, G. Ravikanth, S. Shivashankar, A. Sathish, D. Kun, T. H. Donald, *Nanotechnology* **2006**, *17*, R14.
[27] a) B. Li, W. Han, B. Jiang, Z. Lin, *ACS Nano* **2014**, *8*, 2936–2942; b) W. Han, M. Byun, B. Li, X. Pang, Z. Lin, *Angew. Chem. Int. Ed.* **2012**, *51*, 12588–12592; *Angew. Chem.* **2012**, *124*, 12756–12760.
[28] N. J. Halas, S. Lal, W.-S. Chang, S. Link, P. Nordlander, *Chem. Rev.* **2011**, *111*, 3913–3961.

Received: December 29, 2014
Published online: February 16, 2015

